



# 1 Variation and Trend of Nitrate radical reactivity towards 2 volatile organic compounds in Beijing, China

3

4 Hejun Hu<sup>1</sup>, Haichao Wang<sup>1,2\*</sup>, Keding Lu<sup>3\*</sup>, Jie Wang<sup>1</sup>, Zelong Zheng<sup>1</sup>, Xuezheng Xu<sup>1</sup>, Tianyu Zhai<sup>3</sup>,  
5 Xiaorui Chen<sup>4</sup>, Xiao Lu<sup>1,2</sup>, Momei Qin<sup>5</sup>, Xin Li<sup>3</sup>, Limin Zeng<sup>3</sup>, Min Hu<sup>3</sup>, Yuanhang Zhang<sup>3</sup>

6 <sup>1</sup>School of Atmospheric Sciences, Sun Yat-sen University, and Southern Marine Science and  
7 Engineering Guangdong Laboratory (Zhuhai), Zhuhai, 519082, China

8 <sup>2</sup>Guangdong Provincial Observation and Research Station for Climate Environment and Air Quality  
9 Change in the Pearl River Estuary, Key Laboratory of Tropical Atmosphere-Ocean System (Sun  
10 Yat-sen University), Ministry of Education, Zhuhai, 519082, China

11 <sup>3</sup>State Key Joint Laboratory of Environmental Simulation and Pollution Control, The State  
12 Environmental Protection Key Laboratory of Atmospheric Ozone Pollution Control, College of  
13 Environmental Sciences and Engineering, Peking University, Beijing, 100871, China.

14 <sup>4</sup>Department of Civil and Environmental Engineering, The Hong Kong Polytechnic University, Hong  
15 Kong, China

16 <sup>5</sup>Jiangsu Key Laboratory of Atmospheric Environment Monitoring and Pollution Control,  
17 Collaborative Innovation Center of Atmospheric Environment and Equipment Technology, Nanjing  
18 University of Information Science and Technology, Nanjing, China

19 *Correspondence to:* Haichao Wang (wanghch27@mail.sysu.edu.cn), Keding Lu (k.lu@pku.edu.cn)

20

21 **ABSTRACT.** Nitrate radical (NO<sub>3</sub>) is an important nocturnal atmospheric oxidant in the troposphere,  
22 which significantly affects the lifetime of pollutants emitted by anthropogenic and biological  
23 activities, especially volatile organic compounds (VOC). Here, we used one-year VOC observation  
24 data obtained in urban Beijing in 2019 to look insight to the level, compositions and seasonal  
25 variation of NO<sub>3</sub> reactivity ( $k_{\text{NO}_3}$ ). We show the hourly  $k_{\text{NO}_3}$  towards measured VOC highly varied  
26 from  $<10^{-4}$  to  $0.083 \text{ s}^{-1}$  with campaign-averaged value ( $\pm$  standard deviation) of  $0.0032 \pm 0.0042 \text{ s}^{-1}$ .  
27 There was large seasonal difference in NO<sub>3</sub> reactivity towards VOC with the average of  $0.0024 \pm$   
28  $0.0026 \text{ s}^{-1}$ ,  $0.0067 \pm 0.0066 \text{ s}^{-1}$ ,  $0.0042 \pm 0.0037 \text{ s}^{-1}$ ,  $0.0027 \pm 0.0028 \text{ s}^{-1}$  from spring to winter.  
29 Alkenes such as isoprene and styrene accounted for the majority. Isoprene was the dominant species  
30 in spring, summer, and autumn, accounting for 40.0%, 77.2% and 43.2%, respectively. Styrene only  
31 played a leading role in winter with the percentage of 39.8%. Sensitivity study shows monoterpenes,  
32 the species we did not measure, may account a large fraction of  $k_{\text{NO}_3}$ . Based on the correlation  
33 between the calculated  $k_{\text{NO}_3}$  and VOC concentrations in 2019, we established localized  
34 parameterization schemes for predicting the reactivity by only using a part of VOC species. The  
35 historical published VOC data was collected to reconstruct the long-term NO<sub>3</sub> reactivity in Beijing  
36 by the parameterization method. The downward trend of  $k_{\text{NO}_3}$  during 2011-2020 may be responded to  
37 the reduction of anthropogenic VOC emission. At last, we revealed that NO<sub>3</sub> dominated the nocturnal  
38 VOC oxidation with 83% on the annual average in Beijing in 2019, which varied seasonally and was  
39 strongly regulated by the level of  $k_{\text{NO}_3}$ , nitrogen oxide and ozone. Our results improve the

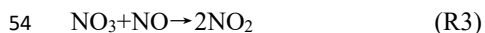
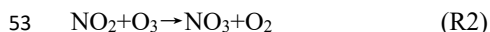
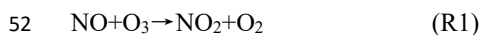


40 understanding of nocturnal atmospheric oxidation in urban regions, and gain the knowledge of  
41 nocturnal VOC oxidation and secondary organic pollution.

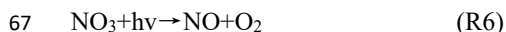
42

### 43 1. Introduction

44 Nitrate radical ( $\text{NO}_3$ ) is the main nocturnal tropospheric oxidant (Brown and Stutz, 2012; Wayne et  
45 al., 1991), which is mainly formed in the reaction of  $\text{NO}_2$  and  $\text{O}_3$ . During the daytime, a large amount  
46 of  $\text{NO}$  emitted by cities is oxidized into  $\text{NO}_2$  by ozone and released into the atmosphere (R1), and  
47  $\text{NO}_2$  continues to be oxidized into  $\text{NO}_3$  by  $\text{O}_3$  (R2).  $\text{NO}_3$  only presents a high concentration level at  
48 night because it has a rapid photolysis rate during the daytime (Stark et al., 2007).  $\text{NO}_3$  can oxidize  
49  $\text{NO}$  into  $\text{NO}_2$  (R3). During the nighttime,  $\text{NO}_3$  and  $\text{NO}_2$  react to form nitrous pentoxide ( $\text{N}_2\text{O}_5$ ) (R4),  
50 and  $\text{N}_2\text{O}_5$  can be decomposed to  $\text{NO}_3$  and  $\text{NO}_2$  (R5), establishing a temperature-dependent  
51 equilibrium.



57 The main removal of  $\text{NO}_3$  from the gas phase is the reaction with  $\text{NO}$  (R3), solar photolysis (R6, R7),  
58 and volatile organic compounds oxidation (R8), forming complex products. In addition,  $\text{NO}_3$  can be  
59 transformed into  $\text{N}_2\text{O}_5$  and removed by heterogeneous hydrolysis (R9), providing an effective way to  
60 remove  $\text{NO}_x$  and produce nitrate aerosol and nitryl chloride (Brown et al., 2004; Dentener and Crutz,  
61 1993; Osthoff et al., 2008). The competition between R8 and R9 determines the fate of nocturnal  
62 nitrogen oxidation chemistry, which leads to the formation of different type secondary pollutants  
63 (Bertram and Thornton, 2009; Brown et al., 2006). Specifically, the degradation of VOC by  $\text{NO}_3$ ,  
64 especially biogenic VOC (Ng et al., 2017), has been proven to be related to the formation of organic  
65 nitrate and secondary organic aerosols (SOA) (Goldstein and Galbally, 2009; Kiendler-Scharr et al.,  
66 2016).



71 The high  $\text{NO}_3$  concentration and fast reaction rate make  $\text{NO}_3$  responsible for the sink of many



72 unsaturated hydrocarbons at night (Edwards et al., 2017; Ng et al., 2017; Yang et al., 2020). The NO<sub>3</sub>  
73 reactivity ( $k_{NO_3}$ ) towards VOC can be calculated by Eq. 1.

$$74 \quad k_{NO_3} = \sum k_i \times [VOC_i] \quad \text{Eq. 1}$$

75 where the  $[VOC_i]$  is VOC concentrations and  $k_i$  is the corresponding reaction rate coefficients. Table  
76 S1 gives the reaction rate coefficients of NO<sub>3</sub> with VOC (Atkinson and Arey, 2003). The NO<sub>3</sub>  
77 reactivity towards different VOC varies greatly, which is affected by the abundance of species and  
78 the reaction rate coefficients. NO<sub>3</sub> reactivity towards VOC is also affected by temperature. Since  
79 temperature not only affects the reaction rate coefficients but also the VOC concentrations in the  
80 atmosphere, especially for the emission of biogenic VOC like isoprene and monoterpenes (Wu et al.,  
81 2020), causing the variations of VOC species which dominate  $k_{NO_3}$  towards VOC in different  
82 seasons.

83 The VOC species which dominant the NO<sub>3</sub> reactivity vary greatly between different regions. In  
84 forests and rural areas, such as Pabstchum outside Berlin, Germany, the lush forests emit a large  
85 amount of monoterpenes and isoprene, accounting for the majority of  $k_{NO_3}$ , which ranged from  
86 0.0025 to 0.01 s<sup>-1</sup> (Asaf et al., 2009); In semi-arid urban areas such as Jerusalem, the emissions of  
87 BVOC are less due to the sparser vegetation, and the maximum of NO<sub>3</sub> reactivity was about 0.01 s<sup>-1</sup>.  
88 Phenol, cresol and some monoolefins emitted by road traffic are the main contributors (Asaf et al.,  
89 2009). In the urban regions like Houston, the industrial emissions including isoprene and other  
90 alkenes dominated the NO<sub>3</sub> reactivity (Stutz et al., 2010). In the suburbs of the city, the  $k_{NO_3}$  may be  
91 jointly affected by anthropogenic and biological volatile organic compounds. For example, the NO<sub>3</sub>  
92 reactivity towards VOC in Xianghe, Beijing reached  $0.024 \pm 0.030$  s<sup>-1</sup>, with the maximum value of  
93 0.3 s<sup>-1</sup> and minimum value of 0.0011 s<sup>-1</sup>. Isoprene, styrene and 2-butene contributed to the majority  
94 of the  $k_{NO_3}$  (Yang et al., 2020).

95 In addition to calculating  $k_{NO_3}$  by the measured VOC, an instrument was developed to directly  
96 measure  $k_{NO_3}$  in the atmosphere (Liebmann et al., 2017). On this basis, they presented the first direct  
97 measurement of NO<sub>3</sub> reactivity in the Finnish boreal forest in 2017 and concluded that the NO<sub>3</sub>  
98 reactivity was generally high with a maximum value of 0.94 s<sup>-1</sup>, displaying a strong diel variation  
99 with nighttime mean value of 0.11 s<sup>-1</sup> and daytime value of 0.04 s<sup>-1</sup> (Liebmann et al., 2018a). In 2018,  
100 they presented the direct measurement in and above the boundary layer of a mountain site, with  
101 daytime values of up to 0.3 s<sup>-1</sup> and nighttime values close to 0.005 s<sup>-1</sup> (Liebmann et al., 2018b). Most  
102 importantly, the direct measurement revealed the existence of missing NO<sub>3</sub> reactivity in varies  
103 regions, which indicated the missing NO<sub>3</sub> oxidation mechanisms, and largely improved the  
104 understanding of nighttime chemistry.

105 Nevertheless, the field direct determination of  $k_{NO_3}$  is still extremely lacked, especially in urban  
106 regions. Until now, most works about the VOC oxidation by NO<sub>3</sub> was usually based on short-term  
107 investigations, and the analysis of nocturnal chemical process or reactivity was carried out based on  
108 the data of a few weeks or several months. The studies of nighttime chemistry based on long-term  
109 measurement data are scarce (Vrekoussis et al., 2007; Wang et al., 2023; Zhu et al., 2022). The  
110 detailed VOC contributions to  $k_{NO_3}$ , and the relationship between certain VOC and total NO<sub>3</sub>  
111 reactivity in a long-time scale are rarely studied. Our recent work reported that the increasing trend



112 of NO<sub>3</sub> production rate caused by the anthropogenic emission changes, while the long-term and  
113 detailed NO<sub>3</sub> loss budget is still uncertain to some extent (Wang et al., 2023). Here, we attempt to  
114 look insight to the level, variations and impacts of NO<sub>3</sub> reactivity by using the one-year measurement  
115 of VOC in an urban site in Beijing, the role of unmeasured VOC species (monoterpenes) in the  
116 contributions of NO<sub>3</sub> reactivity is also discussed. The long-term trend of NO<sub>3</sub> reactivity is estimated  
117 by collecting the published VOC data and the proposed parameterization method. At last, the  
118 regulation of NO<sub>3</sub> oxidation of nocturnal VOC in different seasons is further evaluated.

## 119 2. Methods

### 120 2.1 Site description and instrumentation

121 The measurement was conducted at the campus of Peking University (39° 99' N, 116° 30' E). The  
122 site is situated northeast of the Beijing city center and near two traffic roads, which represents a  
123 typical urban and polluted area with fresh, anthropogenic emissions (Wang et al., 2017a). The  
124 measurements were made on a building roof with a height of 20 m above the ground. Measurements  
125 of VOC concentrations were performed using an automated gas chromatograph equipped with mass  
126 spectrometry or flame ionization detectors (GC-MS/FID). There are 56 kinds of VOC are measured  
127 in total, in which monoterpenes are not valid. NO<sub>x</sub> and O<sub>3</sub> were monitored by chemiluminescence  
128 (Thermo Scientific, 42i-TLE) and UV photometric methods (Thermo Scientific, 49i), respectively. A  
129 Tapered Element Oscillating Microbalance analyzer (TianHong, TH-2000Z1) was used to measure  
130 the mass concentration of PM<sub>2.5</sub>. The quality assurance and quality controls of data were  
131 implemented regularly (Chen et al., 2020). Photolysis frequencies were obtained by the Tropospheric  
132 Ultraviolet and Visible (TUV) model simulation. Hourly data were processed and used in the  
133 following analysis.

### 134 2.2 Estimation of monoterpenes

135 Since the measurement data did not include monoterpenes (MNTs), we therefore use the measured  
136 isoprene and modelled concentration ratio of monoterpene to isoprene in the same region of  
137 measurement site (named as Factor, Eq. 2) to estimate the ambient monoterpene concentrations (Eq.  
138 3). The Factor was obtained by the regional model (WRF/CMAQ), more details of the model  
139 simulation setup can be found in Mao et al. (2022). We used the Factor to estimate monoterpenes  
140 level rather than modelled monoterpene concentrations is due to the modelled isoprene is  
141 systematically higher than that of observation (Fig. S1), thus the using of the modelled Factor may be  
142 more reasonable. In Beijing,  $\alpha$ -pinene and  $\beta$ -pinene were reported to have the highest abundance  
143 among monoterpenes (Cheng et al., 2018), with higher emissions in summer (Wang et al., 2018b;  
144 Xia and Xiao, 2019). Therefore, we approximated the averaged value of  $\alpha$ -pinene and  $\beta$ -pinene  
145 reaction rate coefficients with NO<sub>3</sub> in the following calculations. Since the emissions of  
146 sesquiterpenes in BVOC are much lower than that of isoprene, monoterpenes and other BVOC, we  
147 didn't consider NO<sub>3</sub> reactivity towards sesquiterpenes.

$$148 \quad \text{Factor} = \frac{[MNT_{sim}]}{[ISO_{sim}]} \quad \text{Eq. 2}$$

$$149 \quad [MNT_{obs}] = [ISO_{obs}] \times \text{Factor} \quad \text{Eq. 3}$$



### 150 2.3 VOC oxidation rate by NO<sub>3</sub>

151 To study the reaction of NO<sub>3</sub> and VOC during the nighttime, we estimated the NO<sub>3</sub> concentrations by  
 152 steady-state calculation. This method is widely used to estimate the concentrations of short-lived  
 153 substances like NO<sub>3</sub>, assuming its production and loss rates are balanced in a specific time range.  
 154 Given sufficient time, the steady state can be reached for NO<sub>3</sub> at night in which the production and  
 155 loss terms are approximately balanced (Brown, 2003; Crowley et al., 2010). The production terms of  
 156 NO<sub>3</sub> is the reaction of NO<sub>2</sub> and O<sub>3</sub>, and the loss terms of NO<sub>3</sub> includes reactions with VOC, reaction  
 157 with NO, heterogeneous reaction, and photolysis. The steady-state NO<sub>3</sub> mixing ratios are expressed  
 158 by Eq. 4 (Brown and Stutz, 2012).

$$159 \quad [NO_3]_{ss} = \frac{k_{NO_2+O_3}[NO_2][O_3]}{\sum k_i \times [VOC_i] + k_{NO+NO_3}[NO] + J_{NO_3} + k_{het} K_{eq}[NO_2]} \quad \text{Eq. 4}$$

160 Where  $J_{NO_3}$  is the sum of the photolysis coefficients of the two photolysis reactions of NO<sub>3</sub>. The  $k_{het}$   
 161 is the heterogeneous uptake rate of N<sub>2</sub>O<sub>5</sub> on the aerosol surface, which can be calculated by Eq. 5.

$$162 \quad k_{het} = 0.25 \times \gamma \times S_a \times c \quad \text{Eq. 5}$$

163 Where  $\gamma$  is the dimensionless uptake coefficient of N<sub>2</sub>O<sub>5</sub> parameterized by Eq. 6 (Evans and Jacob,  
 164 2005; Hallquist et al., 2003; Kane et al., 2001),  $S_a$  (m<sup>2</sup> m<sup>-3</sup>) is the aerosol surface area density  
 165 estimated by the level of PM<sub>2.5</sub> (Wang et al., 2021), and  $c$  is the mean molecular velocity of N<sub>2</sub>O<sub>5</sub>.

$$166 \quad \gamma = \alpha \times 10^\beta$$

$$167 \quad \alpha = 2.79 \times 10^{-4} + 1.3 \times 10^{-4} \times RH - 3.43 \times 10^{-6} \times RH^2 + 7.52 \times 10^{-8} \times RH^3$$

$$168 \quad \beta = 4 \times 10^{-2} \times (T - 294) \quad (T > 282K)$$

$$169 \quad \beta = -0.48 \quad (T < 282K) \quad \text{Eq. 6}$$

170 The reaction rate coefficients of NO<sub>2</sub> and O<sub>3</sub>, NO and NO<sub>3</sub>, and the equilibrium constant for the  
 171 forward and reverse Reactions (R4) and (R5) are temperature dependent. We have adopted JPL  
 172 evaluation reports for the reaction rate coefficients. The time series of hourly related parameters in  
 173 estimating the steady-state NO<sub>3</sub> and the diurnal cycle of NO<sub>3</sub> concentrations were shown in Fig. S2  
 174 and Fig. S3. To compare the oxidation of NO<sub>3</sub> towards VOC with other oxidants, we estimated OH  
 175 concentrations by the slope that extracted from the measured OH and  $J_{O1D}$  (s<sup>-1</sup>) in North China (Tan  
 176 et al., 2017)) (Eq. 7), where  $J_{O1D}$  was obtained by the TUV model simulations. The VOC oxidation  
 177 rate and the ratio of VOC oxidized by NO<sub>3</sub> to the total oxidation rate can be calculated by Eq. 8.

$$178 \quad [OH] = 4.1 \times 10^{11} \text{ cm}^{-3} \text{ s}^{-1} \times J_{O1D} \quad \text{Eq. 7}$$

$$179 \quad R_{NO_3} \approx \frac{\sum k_i \times [VOC_i] [NO_3]}{\sum k_i \times [VOC_i] [OH] + \sum k_i \times [VOC_i] [NO_3] + \sum k_i \times [VOC_i] [O_3]} \quad \text{Eq. 8}$$

180 where  $k_i$  represents the corresponding reaction rate coefficients of different VOC with oxidants.

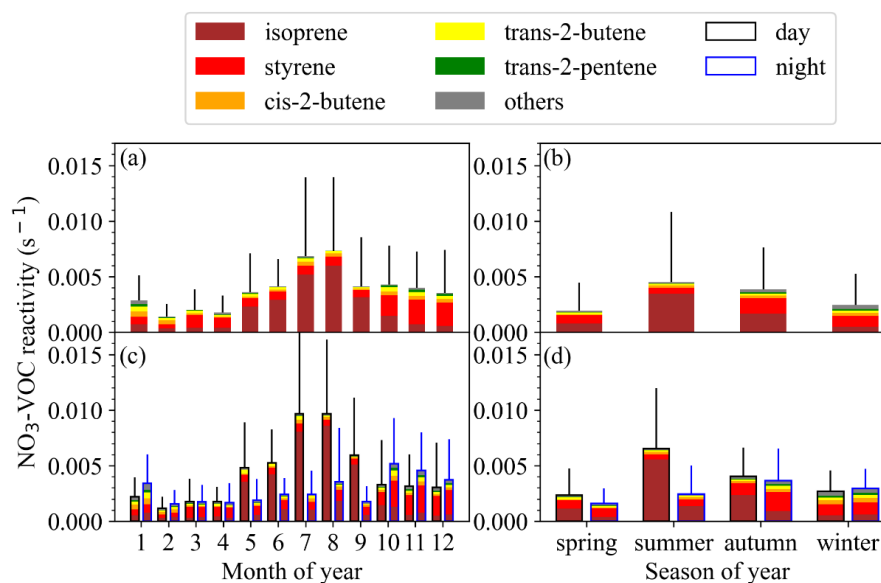


### 181 3. Results and discussion

#### 182 3.1 NO<sub>3</sub> reactivity calculated by measured VOC

183 During the campaign, the hourly  $k_{\text{NO}_3}$  towards measured VOC (named as  $k_{\text{NO}_3_{\text{mea}}}$ ) highly varied  
184 from  $<10^{-4}$  to  $0.083 \text{ s}^{-1}$  with campaign-averaged value ( $\pm$  standard deviation) of  $0.0032 \pm 0.0042 \text{ s}^{-1}$ .  
185 The  $k_{\text{NO}_3_{\text{mea}}}$  displayed a strong diel variation on annual average (Fig. S4). In previous studies, the  
186 NO<sub>3</sub> reactivity towards VOC was reported to be  $0.024 \pm 0.030 \text{ s}^{-1}$  on average in a suburban site in  
187 summer in North China (Yang et al., 2020); and highly varied between  $0.005 - 0.3 \text{ s}^{-1}$  in mountaintop  
188 site in summer (Liebmann et al., 2018c). Our result is one order of magnitude lower, which may  
189 reflect the huge difference of  $k_{\text{NO}_3_{\text{mea}}}$  in different environment and sampling time. Certainly, it may  
190 be attributed to the calculated  $k_{\text{NO}_3}$  here did not include some species, such as monoterpenes. The  
191 diurnal variations of  $k_{\text{NO}_3_{\text{mea}}}$  had strong seasonal variability (Fig. S5). The diurnal variations in  
192 winter and spring were relatively weak, and the variations in summer and autumn were large, with  
193 clear peaks at 9:00-10:00 and 15:00, respectively. The  $k_{\text{NO}_3_{\text{mea}}}$  in spring, summer and autumn  
194 reached the daily maximum value between 8:00 a.m. and 10:00 a.m. (spring:  $0.0034 \text{ s}^{-1}$ , summer:  
195  $0.0083 \text{ s}^{-1}$ , autumn:  $0.0057 \text{ s}^{-1}$ ). In winter, it reached the maximum value of  $0.0033 \text{ s}^{-1}$  at about 22:00.

196 As shown in Fig. 1a, the  $k_{\text{NO}_3_{\text{mea}}}$  reached the highest in August and lowest in February, which was  
197 largely affected by the level of isoprene and styrene. For example, isoprene contributed  $\sim 80\%$  to the  
198 reactivity in August. The  $k_{\text{NO}_3_{\text{mea}}}$  towards isoprene reached the maximum in August and the  
199 minimum in February, which was consistent with the previous reported change of isoprene  
200 concentrations in Beijing (Cheng et al., 2018). Figure 1b shows a large seasonal difference in  
201  $k_{\text{NO}_3_{\text{mea}}}$  with the average value of  $0.0024 \pm 0.0026 \text{ s}^{-1}$ ,  $0.0067 \pm 0.0066 \text{ s}^{-1}$ ,  $0.0042 \pm 0.0037 \text{ s}^{-1}$ ,  
202  $0.0027 \pm 0.0028 \text{ s}^{-1}$  from spring to winter. Table S2 shows the specific contributions of top six  
203 species to  $k_{\text{NO}_3_{\text{mea}}}$  in different seasons (and Fig. S4). Isoprene was the dominant species, accounting  
204 for 40.0%, 77.2% and 43.2% in spring, summer, and autumn. By comparison, styrene only played a  
205 leading role in winter, accounting for 39.8%. Of the species which contributed to  $k_{\text{NO}_3_{\text{mea}}}$  in Beijing,  
206 isoprene and styrene contributed most to the overall  $k_{\text{NO}_3_{\text{mea}}}$  (60%~90%) followed by cis-2-butene,  
207 trans-2-butene, trans-2-pentene and propylene (5%~15%) with another individual VOC less than 2%.  
208 Our results are consistent with previous studies in Beijing that  $k_{\text{NO}_3}$  was mainly contributed by  
209 isoprene (Yang et al., 2020), indicating that the critical role of isoprene in NO<sub>3</sub> reactivity in Beijing.  
210 From summer to autumn, the dominant species changed from isoprene to styrene, while from winter  
211 to spring, the dominant species changed from styrene to isoprene. This indicated the AVOC and  
212 BVOC controls  $k_{\text{NO}_3_{\text{mea}}}$  alternately. Overall, the  $k_{\text{NO}_3_{\text{mea}}}$  displayed a characteristic of high in summer  
213 and autumn and low in winter and spring.



214

215 **Figure 1.** (a-b) Histograms of monthly and seasonal-averaged  $k_{\text{NO}_3\text{-mea}}$  and the compositions. (c-d)  
 216 Histograms of monthly and seasonal-averaged  $k_{\text{NO}_3\text{-mea}}$  and the compositions divided into daytime  
 217 (black frames) and nighttime (blue frames). The color denotes the contributions of different VOC  
 218 species. The black and blue lines represent the error bars of the reactivity ( $\pm$  standard deviations).

219 Figure 1c-d showed the  $k_{\text{NO}_3\text{-mea}}$  towards measured VOC display clear day-night differences in  
 220 summer and winter, especially in summer. The  $\text{NO}_3$  reactivity towards VOC in the daytime reached  
 221 the value of  $0.010 \text{ s}^{-1}$  in July and August, which was much higher than  $0.002 \text{ s}^{-1}$  in the nighttime. The  
 222 variations were mainly caused by the diel variations of isoprene concentrations. Reversely, the  
 223 reactivity was higher at night and lower in the daytime in winter, which was due to the high AVOC  
 224 level in the morning and at night (Lee and Wang, 2006). Specifically, styrene concentrations at night  
 225 increased significantly in the stable nocturnal boundary layer, resulting in relatively higher reactivity.

226 In urban areas of Beijing, isoprene origins from anthropogenic and biological sources, in which the  
 227 anthropogenic sources of isoprene are mainly traffic emissions (Li et al., 2013; Riba et al., 1987; Zou  
 228 et al., 2015). In summer, isoprene mainly origins from plant, and in winter origins from the  
 229 combustion of engine fuel. In spring and autumn, there are mixed effects of anthropogenic and  
 230 biological origins (Li et al., 2013). The isoprene emissions of biological sources in Beijing were one  
 231 order of magnitude larger than that of anthropogenic sources (Yuan et al., 2009). This indicates the  
 232 concentrations of isoprene at the environmental level in the urban areas of Beijing is not affected by  
 233 the traffic vehicles, but mainly by plants in Beijing (Cheng et al., 2018). As an aromatic hydrocarbon,  
 234 styrene origins from both anthropogenic and biogenic sources in the atmosphere (Miller et al., 1994;  
 235 Mogel et al., 2011; Schaeffer et al., 1996; Tang et al., 2000; Zielinska et al., 1996; Zilli et al., 2001),  
 236 such as the laminar flame of engine fuel (Meng et al., 2016), industrial production (Radica et al.,  
 237 2021) and other human activities. The dominant source of styrene in Beijing is the local vehicles  
 238 emissions (Li et al., 2014). Some vegetation, such as evergreen and oleander, can release natural



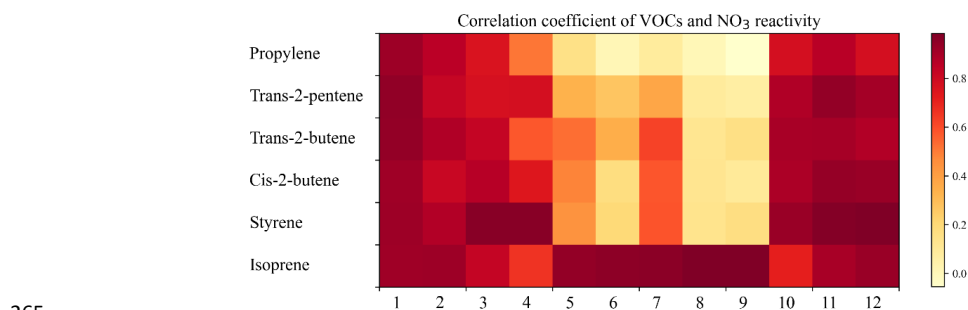
239 styrene (Wu et al., 2014), however, due to the dense industrial distribution in the urban area and the  
 240 much lower level of these biogenic styrene compared with isoprene, we believed that the styrene in  
 241 the atmosphere in Beijing is mainly resulted from anthropogenic origins. It is believed that human  
 242 activities in winter, such as heating, gasoline and diesel combustion increased, meanwhile, the  
 243 reduction of temperature and radiation resulted in the reduction of biogenic isoprene emissions,  
 244 explained the conversion of dominance of NO<sub>3</sub> reactivity from summer to winter.

### 245 3.2 Parameterization of NO<sub>3</sub> reactivity

246 We examined the correlation of key VOC concentrations and  $k_{\text{NO}_3\_mea}$ . Figure S6 gives the case in  
 247 January for example. To a certain extent, the variations of  $k_{\text{NO}_3\_mea}$  were closely linked to the  
 248 variations of the concentrations of main contributors. It is worth noting that in January,  
 249 trans-2-butene had a higher correlation coefficient with  $k_{\text{NO}_3\_mea}$ , which exceeded that of isoprene and  
 250 styrene. This indicates that higher contributions may not imply stronger correlation. Fig. 2 shows the  
 251 correlation coefficients and the fitting equations between VOC concentrations and  $k_{\text{NO}_3}$  in each  
 252 month (detailed in Table S3). According to the correlation coefficients, we can select the strongest  
 253 indicator corresponding to the certain month as the variable of the parameterization method. Here we  
 254 didn't import the VOC with small contributions into the parameterization method, because these  
 255 indicators had no practical significance for  $k_{\text{NO}_3\_mea}$ . In this way, we established the first  
 256 parameterization method by using the strongest indicator in each month and can be found in Table S3  
 257 (Eq. 10):

$$258 \quad \text{NO}_3 \text{ reactivity}_{sim1} = a_i \times [\text{VOC}_i] + b_i \quad \text{Eq. 10}$$

259 where,  $a_i$ ,  $b_i$  and  $[\text{VOC}_i]$  respectively represent the slope, the intercept and the VOC species  
 260 concentrations (ppbv) used for parameterization in each month. Throughout the year, the correlation  
 261 coefficients between isoprene concentrations and  $k_{\text{NO}_3\_mea}$  were high, ranging from 0.67 to 0.98,  
 262 especially in summer. The correlation coefficients between styrene concentrations and the reactivity  
 263 reached a maximum in autumn and winter, which can clearly display the indication of these two  
 264 species (isoprene and styrene) in different seasons.



265

266 **Figure 2.** The thermodynamic diagram of the correlation between VOC concentrations and  $k_{\text{NO}_3\_mea}$ .  
 267 Colored blocks indicate different correlations, by which the best indicator can be selected for  
 268 parameterization method of each month.



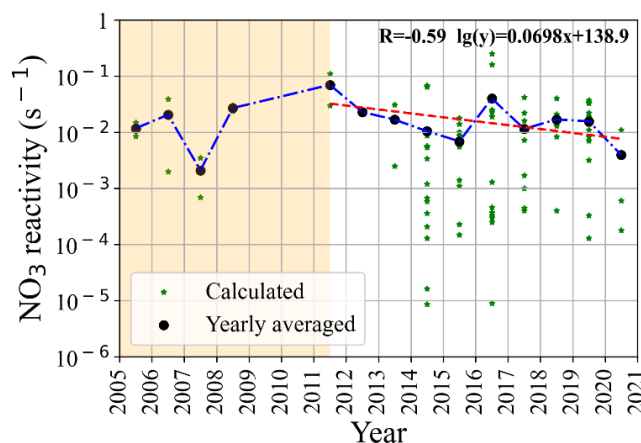
269 Besides the indicator parameterization method, we can also select only a part of VOC that contribute  
270 most of  $k_{\text{NO}_3\text{_{mea}}}$  as a representative. Here we approximated  $\text{NO}_3$  reactivity towards total VOC to the  
271 reactivity towards these top 6 species, namely isoprene, styrene, cis-2-butene, trans-2-butene,  
272 trans-2-pentene and propylene. Thus, the second parameterization method can be expressed by Eq.  
273 11:

$$274 \quad \text{NO}_3 \text{ reactivity}_{\text{sim2}} = \sum_{i=1}^6 k_i \times [\text{VOC}_i] \quad \text{Eq. 11}$$

275 where  $[\text{VOC}_i]$  is the VOC concentrations and  $k_i$  is the corresponding reaction rate coefficients with  
276  $\text{NO}_3$ . It should be noted that this parameterization method of  $\text{NO}_3$  reactivity towards VOC may be  
277 localized.

278 To evaluate the effectiveness of the two parameterization methods established above, we estimated  
279 the  $k_{\text{NO}_3}$  in the different time scale, and compared them with the determined  $k_{\text{NO}_3\text{_{mea}}}$  by all measured  
280 VOC. As shown in Fig. S7, both two methods can well capture the level and variations of  $k_{\text{NO}_3\text{_{mea}}}$ ,  
281 indicating the parameterization feasibility. Method 1 can easily and quickly estimate  $\text{NO}_3$  reactivity  
282 towards VOC by using a single indicator. In areas where  $\text{NO}_3$  reactivity towards VOC is dominated  
283 by a single VOC specie for a long time, such as forest areas, suburbs, rural areas (BVOC dominant),  
284 this method would have a good performance. Method 2 had a better performance while more VOC  
285 species are needed. In urban areas, especially in urban areas where the contributors had different  
286 chemo diversity with strong seasonality, this method should be more suitable. Since the two methods  
287 lower the bar for estimating  $\text{NO}_3$  reactivity by using VOC measurement data, we can look into the  
288 level of  $\text{NO}_3$  reactivity by using the reported VOC measurement data in the past.

289 We collected the historical measurement data of VOC concentrations in Beijing (Supporting file. S1)  
290 and estimated  $\text{NO}_3$  reactivity by the parameterization methods. We found the level of  $\text{NO}_3$  reactivity  
291 mainly ranged from 0.001 to 0.1  $\text{s}^{-1}$  in Beijing in the past decades (Fig. 3). Due to the limitation of  
292 data, we cannot find a trend of  $\text{NO}_3$  reactivity before 2011. While during 2011-2020, large amount of  
293 VOC data in urban Beijing presented and be collected in this study. We calculated the  $k_{\text{NO}_3\text{_{mea}}}$  by  
294 detailed VOC with respect to the data provided by the literatures, and estimated the  $\text{NO}_3$  reactivity by  
295 parameterization methods if the reported data in the literatures is limited. As shown in Fig. 3, an  
296 overall decrease trend of  $\text{NO}_3$  reactivity can be found during 2011-2020. We inferred that the level of  
297 isoprene during this period may be varied small, since the biogenic emission unlikely to change  
298 much. Thus, we proposed that the decrease of  $\text{NO}_3$  reactivity during the past decade may be  
299 attributed to the anthropogenic emission reduction of anthropogenic VOC. It should be noted that  
300 this estimation suffers from the uncertainty, nevertheless, this trend and characterization of  $\text{NO}_3$   
301 reactivity in Beijing is helpful to understand the nighttime chemistry in Beijing.



302

303 **Figure 3.** The reconstructed NO<sub>3</sub> reactivity calculated by the reported VOC concentrations in Beijing.  
 304 The averaged NO<sub>3</sub> reactivity calculated by the reported VOC data in each campaign plotted as star.  
 305 The yearly averaged NO<sub>3</sub> reactivity (black dot) between 2011-2019 shows a decline. It should be  
 306 noted that the monoterpenes are not considered here.

### 307 3.3 NO<sub>3</sub> reactivity towards monoterpenes

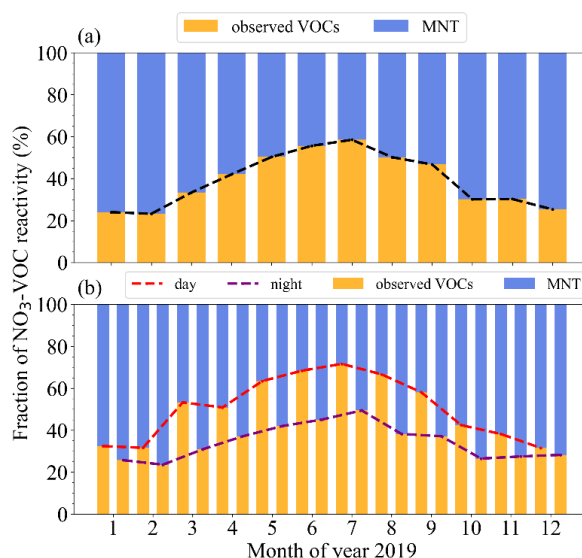
308 After taking MNTs into account, the total  $k_{\text{NO}_3}$  (named as  $k_{\text{NO}_3_{\text{total}}}$ ) was greatly enlarged, with  
 309 campaign-averaged value of  $0.0061 \pm 0.0088 \text{ s}^{-1}$ , resulting in our results comparable with previous  
 310 research results. The NO<sub>3</sub> reactivity towards MNTs (named as  $k_{\text{NO}_3_{\text{MNTs}}}$ ) was higher in autumn and  
 311 winter and lower in spring and summer (Fig. S8). Considering the corresponding reactivity towards  
 312 monoterpenes, the total NO<sub>3</sub> reactivity towards VOC changed from (summer > autumn > winter >  
 313 spring) to (autumn > winter > summer > spring), highlights the impact of the monoterpene variations  
 314 on the reactivity. The NO<sub>3</sub> reactivity towards MNTs displayed significant differences between  
 315 daytime and nighttime (Fig. S8c-d). The reactivity at night in all months was higher than that in the  
 316 daytime, especially from October to January, highlights the role of biogenic monoterpenes in  
 317 nocturnal NO<sub>3</sub> chemistry (Li et al., 2013; Riba et al., 1987). To compare the measured and the total  
 318 NO<sub>3</sub> reactivity towards VOC, we calculated the fraction ( $F_{\text{MNTs}}$ ) by Eq. 12.

$$319 \quad F_{\text{MNTs}} = \frac{k_{\text{NO}_3_{\text{MNTs}}}}{k_{\text{NO}_3_{\text{total}}}} \quad \text{Eq. 12}$$

320 Figure 4a displays the differences between the  $k_{\text{NO}_3_{\text{mea}}}$  and  $k_{\text{NO}_3_{\text{total}}}$ . Monoterpenes were very  
 321 important for NO<sub>3</sub> reactivity, and the  $F_{\text{MNTs}}$  varied from 40% to 80%, with strong seasonal variations.  
 322 The MNTs accounted for NO<sub>3</sub> reactivity nearly 80% in winter and spring. In the seasons when  
 323 isoprene no longer dominated, the measured reactivity accounted for a small fraction, and the  
 324 corresponding reactivity towards AVOC such as styrene was smaller than that of monoterpenes. As  
 325 shown in Fig. 4b, the measured VOC had high fractions in the daytime and low at night. Especially  
 326 in May and August. The measured VOC in the daytime accounted for more than 60% of  $k_{\text{NO}_3_{\text{total}}}$ ,  
 327 which was closely related to the increasing concentrations of isoprene in the summer daytime. The



328 reactivity towards MNTs accounted for a large fraction of reactivity at night.



329

330 **Figure 4.** (a) Fractions of the  $k_{\text{NO}_3_{\text{total}}}$ . (b) Fractions of the  $k_{\text{NO}_3_{\text{total}}}$  divided into daytime (left) and  
 331 nighttime (right). The colors on the stacked bar plot indicate the different fractions as they are  
 332 donated in the legend. The lines represent the monthly-averaged variations of the  $\text{NO}_3$  reactivity  
 333 towards MNTs.

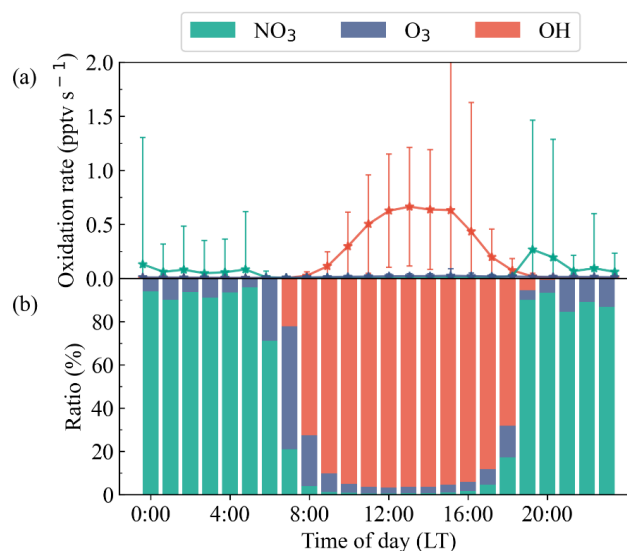
334 We updated the parameterization method established before by using the relationship between  
 335 reactivity and VOC concentrations including monoterpenes. The updated parameterization Method 1  
 336 used the same principle as introduced in Sect 3.2, with fitting slopes changing significantly (Fig. S9).  
 337 Table S4 gives the specific correlation coefficients between six key VOC concentrations and  $k_{\text{NO}_3_{\text{total}}}$ .  
 338 The updated Method 2 considered the sum contributions of six VOC and the estimated MNTs by  
 339 isoprene concentration. We reevaluated the two updated parameterization methods (single VOC and  
 340 six VOC, respectively). Overall, the performance of two methods are reasonable and the updated  
 341 Method 1 is better than that of Method 2 in general (Fig. S10).

### 342 3.4 Nighttime VOC oxidation

343 Here we examined the role of  $\text{NO}_3$  in the VOC oxidation in Beijing 2019. As shown in Fig. 5, OH  
 344 oxidized most of VOC during the daytime, with the oxidation rate reached the maximum value of 0.6  
 345 pptv  $\text{s}^{-1}$  in the afternoon. Compared with OH, the VOC oxidation rates by  $\text{O}_3$  and  $\text{NO}_3$  in the daytime  
 346 were remarkably lower. From 18:00 to 6:00, the characteristics of nocturnal chemical in Beijing were  
 347 significant. The ratios of VOC oxidized by  $\text{NO}_3$  kept above 80%, the contribution of  $\text{O}_3$  was  
 348 relatively weak, which is consistent with that reported in high  $\text{NO}_x$  regions (Chen et al., 2019;  
 349 Edwards et al., 2017; Wang et al., 2018a). The VOC oxidation rate by  $\text{NO}_3$  presented a single peak at  
 350 19:00 with the value of 0.25 pptv  $\text{s}^{-1}$ , which is the same magnitude as that by OH in the daytime,  
 351 illustrating the importance of  $\text{NO}_3$  in VOC oxidation as shown in the previous studies (Wang et al.,



352 2017a), highlight the importance of nocturnal chemistry for organic nitrate and SOA formation.



353

354 **Figure 5.** (a) Median diurnal profile of VOC oxidation rate by OH, NO<sub>3</sub> and O<sub>3</sub>. The colored lines  
355 are error bars (+standard deviation). (b) Fractions of VOC oxidation rate by atmospheric oxidants.

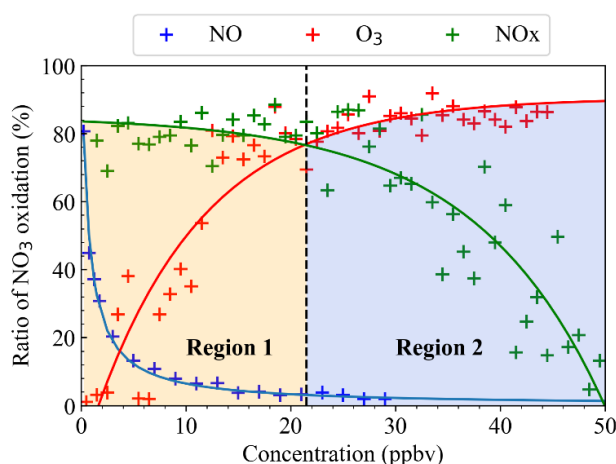
356 The VOC oxidation rate by NO<sub>3</sub> and oxidation fractions had strong seasonal variabilities in Beijing.  
357 As shown in Fig. S11, the nighttime oxidation rate (summer > spring > autumn > winter) was  
358 affected by NO<sub>3</sub> concentrations and the total NO<sub>3</sub> reactivity towards VOC. In summer, the NO<sub>3</sub>  
359 oxidation rate presented a single peak, with a maximum value of 0.7 pptv s<sup>-1</sup> at 20:00, and remained  
360 around 0.1 pptv s<sup>-1</sup> at the rest of the night. The rate at 21:00-5:00 was relatively constant. The rate in  
361 winter was lower, with the two maximum values of 0.06 pptv s<sup>-1</sup> presented at 19:00 and 4:00, which  
362 were further lower than the average value of other three seasons. The results were good agreement  
363 with the previous studies, in which the VOC oxidation rate by NO<sub>3</sub> concentrations contained high  
364 from 19:00-23:00 (Wang et al., 2017b). There was a competition between NO<sub>3</sub> and O<sub>3</sub> in the  
365 nighttime VOC oxidation in Beijing. Although the NO<sub>3</sub> oxidation rate at night was higher than that  
366 of O<sub>3</sub> throughout the year, the changes of O<sub>3</sub> oxidation rate had a significant impact on the ratios of  
367 VOC oxidized by NO<sub>3</sub>. The ratios of nighttime VOC oxidized by NO<sub>3</sub> in Beijing were higher in  
368 autumn, and then in spring, summer and winter. Although the O<sub>3</sub> concentrations in winter decreased,  
369 the competitiveness of NO<sub>3</sub> in VOC oxidation decreased more due to the decline of NO<sub>3</sub>  
370 concentrations. The competitiveness of O<sub>3</sub> in VOC oxidation was relatively enhanced, resulting in a  
371 significant decline in the ratios of VOC oxidized by NO<sub>3</sub>.

### 372 3.5 Regulation of nighttime VOC oxidation

373 To understand the importance of nighttime VOC oxidized by NO<sub>3</sub>, we explored the relationship  
374 between the nocturnal oxidation ratios of NO<sub>3</sub> (R<sub>NO3</sub>) and the nighttime concentrations of NO, O<sub>3</sub>  
375 and NO<sub>x</sub>. It is found that a strong nonlinear relationship between them (shown in Figure 6). The



376  $R_{NO_3}$  had negative correlation coefficients with NO concentrations. With the increase of NO  
 377 concentrations at night, the ratios decreased exponentially. When the NO concentrations increased at  
 378 low NO condition, it could cause a significant decline in the ratios of VOC oxidized by  $NO_3$ . While  
 379 at high NO condition, the ratios were not sensitive to the increase of NO concentrations (Fig. S12),  
 380 indicating that the nighttime NO concentrations in Beijing strongly controlled the ratios effectively. It  
 381 can be expected since the increase of NO concentrations controlled the  $NO_3$  loss term, then caused  
 382 the decrease of  $NO_3$  concentration. When the NO concentrations exceeded a threshold value, the  $NO_3$   
 383 loss was totally dominated by NO.



384

385 **Figure 6.** Fitting diagrams between the ratios of nighttime VOC oxidized by  $NO_3$  and the  
 386 concentrations of NO,  $O_3$  and  $NO_x$ . In Region 1, the ratio is more sensitive to  $O_3$ , while less sensitive  
 387 to  $NO_x$ . In Region 2, it is more sensitive to  $NO_x$ , while less sensitive to  $O_3$ .

388 The ratios of nighttime VOC oxidized by  $NO_3$  also had a strong nonlinear relationship with  $O_3$  and  
 389  $NO_x$  concentrations.  $O_3$  concentrations have one positive and one negative contribution to the  $R_{NO_3}$ .  
 390 The positive effect is that increasing  $O_3$  concentration increase the  $NO_3$  production rate, which  
 391 increase the  $NO_3$  steady-state concentrations then increase the ratios. And the negative is increasing  
 392  $O_3$  concentrations increase the reaction rate between VOC and  $O_3$ , which increase the  
 393 competitiveness of  $O_3$  in VOC oxidation then decrease the ratios. Figure. S12 also shows the  
 394 relationship between the  $R_{NO_3}$  and the concentrations of  $O_3$ . While  $O_3$  concentrations below 21.5  
 395 ppbv, the ratios were very sensitive to  $O_3$  level, which fast increased with  $O_3$  concentrations. While  
 396 the ratio become not sensitive and remained relatively constant when the  $O_3$  concentrations exceeded  
 397 21.5 ppbv. It can be explained that when the  $O_3$  concentrations were low, the  $NO_3$  production rate was  
 398 more sensitive to the increase of  $O_3$  concentrations. In this case,  $O_3$  mainly affects the ratios  
 399 positively. When the  $O_3$  concentrations were high, the positive effect of  $O_3$  tended to be constant,  
 400 indicates the two opposite effects overall keep in balance.

401 When the  $NO_x$  concentrations were low (e.g., <21.5 ppbv), the  $R_{NO_3}$  were less sensitive to  $NO_x$ ,  
 402 remaining relatively constant with the further increase. It is believed that the increase of  $NO_3$  loss



403 rates through the  $\text{N}_2\text{O}_5$  heterogeneous reaction and the NO reaction were kept in balance with the  
404  $\text{NO}_3$  production rate increased by  $\text{NO}_2$  concentrations. At high  $\text{NO}_x$  condition, the ratios sensitively  
405 decreased with the increase of  $\text{NO}_x$  concentrations, which is explained that the increase of  $\text{NO}_3$  loss  
406 rates by NO, resulting in a decline in the ratios.

407 To better understand the nonlinear effect of  $\text{NO}_2$  and  $\text{O}_3$  on the nighttime VOC oxidation, we further  
408 explored the effect of  $\text{O}_3$  concentration on the ratios existing in different concentrations of  $\text{NO}_2$ . As  
409 shown in Fig. S13, in higher concentrations of  $\text{NO}_2$ , the threshold of lower  $\text{O}_3$  concentrations were  
410 required for the  $R_{\text{NO}_3}$  to become constant, which reflected the couple influence of  $\text{NO}_2$  and  $\text{O}_3$  on  
411 nighttime VOC oxidation through the nonlinear response, and indicated that in the environment  
412 richen in  $\text{NO}_2$ , nocturnal  $\text{NO}_3$  chemistry easily tended to be more dominant.

#### 413 4. Conclusions and implications

414 In this study, we showed the  $\text{NO}_3$  reactivity towards measured VOC highly varied with strong  
415 seasonal differences, which was mainly driven by isoprene concentrations. The top 6 contributors to  
416 the measured  $\text{NO}_3$  reactivity towards VOC were isoprene, styrene, cis-2-butene, trans-2-butene,  
417 trans-2-pentene and propylene. Among them, isoprene and styrene contributed most of the reactivity.  
418 In addition, monoterpenes are proposed to be a significant source of  $\text{NO}_3$  reactivity. Recently studies  
419 showed the anthropogenic emissions contributes significantly to the ambient MNTs concentrations  
420 by biomass burning, traffic and volatile chemical product emissions in the urban regions, it would  
421 further enhance the importance of nocturnal  $\text{NO}_3$  oxidation (Coggon et al., 2021; Nelson et al., 2021;  
422 Peng et al., 2022; Qin et al., 2020; Wang et al., 2022). It should be noted that the estimated  
423 contributions of MNTs only considered the biogenic emissions and may be represent the lower bias,  
424 thus we highlight the importance of field observation of MNTs for advancing the understanding the  
425 nighttime  $\text{NO}_3$  chemistry. In addition, it should be noted that we didn't take the contributions of  
426 OVOC into account, since the reaction rate coefficients of OVOC with  $\text{NO}_3$  are small (Ambrose et  
427 al., 2007).

428 Looking insight to the trend and evolution of detailed  $\text{NO}_3$  chemistry is very scare, but it can really  
429 helpful to understand response of the nocturnal chemistry on the emission change at a large time  
430 scale. Limited by the non-extensive and non-continuous observation, we cannot obtain the long-time  
431 measurement of all the VOC species in multiple sites. Since isoprene and styrene are good indicators  
432 of  $\text{NO}_3$  reactivity in different seasons, at least as we shown in urban Beijing, those can be used to  
433 estimate the  $\text{NO}_3$  reactivity towards VOC to reestablish the long-term trend of  $\text{NO}_3$  reactivity in  
434 urban regions for further evaluation of its history of nighttime chemistry. We admitted that the  
435 estimation of  $\text{NO}_3$  reactivity trend may be highly uncertain, but this attempt may be very helpful to  
436 know the level and overall change of nighttime chemistry.

437 We showed that  $\text{NO}_3$  dominated the nighttime VOC oxidation in Beijing, but the oxidation ratio had  
438 a strong nonlinear relationship with  $\text{O}_3$  and  $\text{NO}_x$  concentrations. With the  $\text{NO}_2$  concentrations  
439 decrease, the threshold values of  $\text{O}_3$  between sensitive regime and non-sensitive regime tended to  
440 increase, indicative of the nighttime oxidation by  $\text{NO}_3$  would be more easily affected by the level of  
441  $\text{O}_3$  with the implement of sustaining  $\text{NO}_x$  reduction in the future. The threshold values of  $\text{O}_3$  can  
442 provide an effective basis for the measures to control nocturnal chemical and secondary organic



443 aerosols pollution in the typical urban region.

444 **Code/Data availability.** The datasets used in this study are available from the corresponding author  
445 upon request (wanghch27@mail.sysu.edu.cn; k.lu@pku.edu.cn).

446 **Author contributions.** H.C.W. and K.D.L. designed the study. H.J.H. and H.C.W. analyzed the data  
447 with input from J.W., Z.L.Z., X.Z.X., T.Y.Z., X.R.C., X.L., M.M.Q. provided the modelled  
448 monoterpene and isoprene data, X.L., L.M.Z., M.H., and Y.H.Z. organized this field campaign and  
449 provided the field measurement dataset. H.J.H. and H.C.W. wrote the paper with input from K.D.L.

450 **Competing interests.** The authors declare that they have no conflicts of interest.

451 **Acknowledgments.** This project is supported by the National Natural Science Foundation of China  
452 (42175111, 21976006). Thanks for the data contributed by field campaign team.

453

#### 454 **Reference.**

- 455 Ambrose JL, Mao H, Mayne HR, Stutz J, Talbot R, Sive BC. Nighttime nitrate radical chemistry at Appledore island, Maine  
456 during the 2004 international consortium for atmospheric research on transport and transformation. *Journal of*  
457 *Geophysical Research-Atmospheres* 2007; 112: 19.
- 458 Asaf D, Pedersen D, Matveev V, Peleg M, Kern C, Zingler J, et al. Long-Term Measurements of NO<sub>3</sub> Radical at a Semiarid  
459 Urban Site: 1. Extreme Concentration Events and Their Oxidation Capacity. *Environmental Science &*  
460 *Technology* 2009; 43: 9117-9123.
- 461 Atkinson R, Arey J. Atmospheric degradation of volatile organic compounds. *Chemical Reviews* 2003; 103: 4605-4638.
- 462 Bertram TH, Thornton JA. Toward a general parameterization of N<sub>2</sub>O<sub>5</sub> reactivity on aqueous particles: the competing  
463 effects of particle liquid water, nitrate and chloride. *Atmospheric Chemistry and Physics* 2009; 9: 8351-8363.
- 464 Brown SS. Applicability of the steady state approximation to the interpretation of atmospheric observations of NO<sub>3</sub> and  
465 N<sub>2</sub>O<sub>5</sub>. *Journal of Geophysical Research* 2003; 108.
- 466 Brown SS, Dibb JE, Stark H, Aldener M, Vozella M, Whitlow S, et al. Nighttime removal of NO<sub>x</sub> in the summer marine  
467 boundary layer. *Geophysical Research Letters* 2004; 31: 5.
- 468 Brown SS, Ryerson TB, Wollny AG, Brock CA, Peltier R, Sullivan AP, et al. Variability in nocturnal nitrogen oxide processing  
469 and its role in regional air quality. *Science* 2006; 311: 67-70.
- 470 Brown SS, Stutz J. Nighttime radical observations and chemistry. *Chemical Society Reviews* 2012; 41: 6405-6447.
- 471 Chen X, Wang H, Liu Y, Su R, Wang H, Lou S, et al. Spatial characteristics of the nighttime oxidation capacity in the  
472 Yangtze River Delta, China. *Atmospheric Environment* 2019; 208: 150-157.
- 473 Cheng X, Li H, Zhang YJ, Li YP, Zhang WQ, Wang XZ, et al. Atmospheric isoprene and monoterpenes in a typical urban  
474 area of Beijing: Pollution characterization, chemical reactivity and source identification. *Journal of*  
475 *Environmental Sciences* 2018; 71: 150-167.
- 476 Coggon MM, Gkatzelis GI, McDonald BC, Gilman JB, Schwantes RH, Abuhassan N, et al. Volatile chemical product  
477 emissions enhance ozone and modulate urban chemistry. *Proceedings of the National Academy of Sciences of*  
478 *the United States of America* 2021; 118.
- 479 Crowley JN, Schuster G, Pouvesle N, Parchatka U, Fischer H, Bonn B, et al. Nocturnal nitrogen oxides at a rural  
480 mountain-site in south-western Germany. *Atmospheric Chemistry and Physics* 2010; 10: 2795-2812.
- 481 Dentener FJ, Crutz PJ. Reaction of N<sub>2</sub>O<sub>5</sub> on tropospheric aerosols: impact on the global distributions of NO<sub>x</sub>, O<sub>3</sub>, OH.  
482 *Journal of Geophysical Research* 1993; 98: 7149-7163.



- 483 Edwards PM, Aikin KC, Dube WP, Fry JL, Gilman JB, de Gouw JA, et al. Transition from high- to low-NO<sub>x</sub> control of  
484 night-time oxidation in the southeastern US. *Nature Geoscience* 2017; 10: 490-+.
- 485 Evans MJ, Jacob DJ. Impact of new laboratory studies of N<sub>2</sub>O<sub>5</sub> hydrolysis on global model budgets of tropospheric  
486 nitrogen oxides, ozone, and OH. *Geophysical Research Letters* 2005; 32: 4.
- 487 Goldstein AH, Galbally IE. Known and unexplored organic constituents in the Earth's atmosphere. *Geochimica Et*  
488 *Cosmochimica Acta* 2009; 73: A449-A449.
- 489 Hallquist M, Stewart DJ, Stephenson SK, Cox RA. Hydrolysis of N<sub>2</sub>O<sub>5</sub> on sub-micron sulfate aerosols. *Physical Chemistry*  
490 *Chemical Physics* 2003; 5: 3453-3463.
- 491 Kane SM, Caloz F, Leu MT. Heterogeneous Uptake of Gaseous N<sub>2</sub>O<sub>5</sub> by (NH<sub>4</sub>)<sub>2</sub>SO<sub>4</sub>, NH<sub>4</sub>HSO<sub>4</sub>, and H<sub>2</sub>SO<sub>4</sub> Aerosols. *The*  
492 *Journal of Physical Chemistry A* 2001; 105: 6465-6470.
- 493 Kiendler-Scharr A, Mensah AA, Friese E, Topping D, Nemitz E, Prevot ASH, et al. Ubiquity of organic nitrates from  
494 nighttime chemistry in the European submicron aerosol. *Geophysical Research Letters* 2016; 43: 7735-7744.
- 495 Lee BS, Wang JL. Concentration variation of isoprene and its implications for peak ozone concentration. *Atmospheric*  
496 *Environment* 2006; 40: 5486-5495.
- 497 Li L, Li H, Zhang XM, Wang L, Xu LH, Wang XZ, et al. Pollution characteristics and health risk assessment of benzene  
498 homologues in ambient air in the northeastern urban area of Beijing, China. *Journal of Environmental Sciences*  
499 2014; 26: 214-223.
- 500 Li L, Wu F, Meng X. Seasonal and Diurnal Variation of Isoprene in the Atmosphere of Beijing. *Environmental Monitoring*  
501 *in China* 2013; 29: 120-124.
- 502 Liebmann J, Karu E, Sobanski N, Schuladen J, Ehn M, Schallhart S, et al. Direct measurement of NO<sub>3</sub> radical reactivity in  
503 a boreal forest. *Atmospheric Chemistry and Physics* 2018a; 18: 3799-3815.
- 504 Liebmann JM, Muller JBA, Kubistin D, Claude A, Holla R, Plass-Dulmer C, et al. Direct measurements of NO<sub>3</sub> reactivity in  
505 and above the boundary layer of a mountaintop site: identification of reactive trace gases and comparison with  
506 OH reactivity. *Atmospheric Chemistry and Physics* 2018b; 18: 12045-12059.
- 507 Liebmann JM, Muller JBA, Kubistin D, Claude A, Holla R, Plass-Dülmer C, et al. Direct measurements of  
508 NO<sub>3</sub> reactivity in and above the boundary layer of a mountaintop site: identification of  
509 reactive trace gases and comparison with OH reactivity. *Atmospheric Chemistry and Physics* 2018c; 18:  
510 12045-12059.
- 511 Liebmann JM, Schuster G, Schuladen JB, Sobanski N, Lelieveld J, Crowley JN. Measurement of ambient NO<sub>3</sub> reactivity:  
512 design, characterization and first deployment of a new instrument. *Atmospheric Measurement Techniques*  
513 2017; 10: 1241-1258.
- 514 Mao J, Li L, Li J, Sulaymon ID, Xiong K, Wang K, et al. Evaluation of Long-Term Modeling Fine Particulate Matter and  
515 Ozone in China During 2013–2019. *Frontiers in Environmental Science* 2022; 10.
- 516 Meng X, Hu EJ, Li XT, Huang ZH. Experimental and kinetic study on laminar flame speeds of styrene and ethylbenzene.  
517 *Fuel* 2016; 185: 916-924.
- 518 Miller RR, Newhook R, Poole A. Styrene production, use and human exposure. *Critical Reviews in Toxicology* 1994; 24:  
519 S1-S10.
- 520 Mogel I, Baumann S, Bohme A, Kohajda T, von Bergen M, Simon JC, et al. The aromatic volatile organic compounds  
521 toluene, benzene and styrene induce COX-2 and prostaglandins in human lung epithelial cells via oxidative  
522 stress and p38 MAPK activation. *Toxicology* 2011; 289: 28-37.
- 523 Nelson BS, Stewart GJ, Drysdale WS, Newland MJ, Vaughan AR, Dunmore RE, et al. In situ ozone production is highly  
524 sensitive to volatile organic compounds in Delhi, India. *Atmospheric Chemistry and Physics* 2021; 21:  
525 13609-13630.
- 526 Ng NL, Brown SS, Archibald AT, Atlas E, Cohen RC, Crowley JN, et al. Nitrate radicals and biogenic volatile organic



- 527 compounds: oxidation, mechanisms, and organic aerosol. *Atmospheric Chemistry and Physics* 2017; 17:  
528 2103-2162.
- 529 Osthoff HD, Roberts JM, Ravishankara AR, Williams EJ, Lerner BM, Sommariva R, et al. High levels of nitryl chloride in  
530 the polluted subtropical marine boundary layer. *Nature Geoscience* 2008; 1: 324-328.
- 531 Peng Y, Mouat AP, Hu Y, Li M, McDonald BC, Kaiser J. Source appointment of volatile organic compounds and evaluation  
532 of anthropogenic monoterpene emission estimates in Atlanta, Georgia. *Atmospheric Environment* 2022; 288.
- 533 Qin M, Murphy BN, Isaacs KK, McDonald BC, Lu Q, McKeen SA, et al. Criteria pollutant impacts of volatile chemical  
534 products informed by near-field modelling. *Nature Sustainability* 2020; 4: 129-137.
- 535 Radica F, Della Ventura G, Malfatti L, Guidi MC, D'Arco A, Grilli A, et al. Real-time quantitative detection of styrene in  
536 atmosphere in presence of other volatile-organic compounds using a portable device. *Talanta* 2021; 233: 7.
- 537 Riba ML, Tathy JP, Tsiropoulos N, Monsarrat B, Torres L. Diurnal variation in the concentration of  $\alpha$ - and  $\beta$ -pinene in the  
538 landes forest (France). *Atmospheric Environment* 1987; 21: 191-193.
- 539 Schaeffer V, Bhooshan B, Chen S, Sonenthal J, Hodgson A. Characterization of Volatile Organic Chemical Emissions From  
540 Carpet Cushions. *Journal of the Air & Waste Management Association (1995)* 1996; 46: 813-820.
- 541 Stark H, Lerner BM, Schmitt R, Jakoubek R, Williams EJ, Ryerson TB, et al. Atmospheric in situ measurement of nitrate  
542 radical (NO<sub>3</sub>) and other photolysis rates using spectroradiometry and filter radiometry. *Journal of Geophysical  
543 Research-Atmospheres* 2007; 112: 11.
- 544 Stutz J, Wong KW, Lawrence L, Ziemba L, Flynn JH, Rappengluck B, et al. Nocturnal NO<sub>3</sub> radical chemistry in Houston, TX.  
545 *Atmospheric Environment* 2010; 44: 4099-4106.
- 546 Tan ZF, Fuchs H, Lu KD, Hofzumahaus A, Bohn B, Broch S, et al. Radical chemistry at a rural site (Wangdu) in the North  
547 China Plain: observation and model calculations of OH, HO<sub>2</sub> and RO<sub>2</sub> radicals. *Atmospheric Chemistry and  
548 Physics* 2017; 17: 663-690.
- 549 Tang WC, Hemm I, Eisenbrand G. Estimation of human exposure to styrene and ethylbenzene. *Toxicology* 2000; 144:  
550 39-50.
- 551 Vrekoussis M, Mihalopoulos N, Gerasopoulos E, Kanakidou M, Crutzen PJ, Lelieveld J. Two-years of NO<sub>3</sub> radical  
552 observations in the boundary layer over the Eastern Mediterranean. *Atmospheric Chemistry and Physics* 2007;  
553 7: 315-327.
- 554 Wang H, Lu K, Chen X, Zhu Q, Chen Q, Guo S, et al. High N<sub>2</sub>O<sub>5</sub> Concentrations Observed in Urban Beijing: Implications  
555 of a Large Nitrate Formation Pathway. *Environmental Science & Technology Letters* 2017a; 4: 416-420.
- 556 Wang H, Lu K, Guo S, Wu Z, Shang D, Tan Z, et al. Efficient N<sub>2</sub>O<sub>5</sub> uptake and NO<sub>3</sub> oxidation in the outflow of urban  
557 Beijing. *Atmospheric Chemistry and Physics* 2018a; 18: 9705-9721.
- 558 Wang H, Ma X, Tan Z, Wang H, Chen X, Chen S, et al. Anthropogenic monoterpenes aggravating ozone pollution.  
559 *National Science Review* 2022.
- 560 Wang H, Wang H, Lu X, Lu K, Zhang L, Tham YJ, et al. Increased night-time oxidation over China despite widespread  
561 decrease across the globe. *Nature Geoscience* 2023.
- 562 Wang HC, Lu KD, Chen SY, Li X, Zeng LM, Hu M, et al. Characterizing nitrate radical budget trends in Beijing during  
563 2013-2019. *Science of the Total Environment* 2021; 795: 9.
- 564 Wang HC, Lu KD, Guo S, Wu ZJ, Shang DJ, Tan ZF, et al. Efficient N<sub>2</sub>O<sub>5</sub> uptake and NO<sub>3</sub> oxidation in the outflow of urban  
565 Beijing. *Atmospheric Chemistry and Physics* 2018b; 18: 9705-9721.
- 566 Wang HC, Lu KD, Tan ZF, Sun K, Li X, Hu M, et al. Model simulation of NO<sub>3</sub>, N<sub>2</sub>O<sub>5</sub> and ClNO<sub>2</sub> at a rural site in Beijing  
567 during CAREBeijing-2006. *Atmospheric Research* 2017b; 196: 97-107.
- 568 Wayne RP, Barnes I, Biggs P, Burrows JP, Canosa-Mas CE, Hjorth J, et al. The nitrate radical: physics, chemistry, and the  
569 atmosphere. *Atmospheric Environment, Part A (General Topics)* 1991; 25A: 1-203.
- 570 Wu K, Yang X, Chen D, Gu S, Lu Y, Jiang Q, et al. Estimation of biogenic VOC emissions and their corresponding impact on



- 571 ozone and secondary organic aerosol formation in China. *Atmospheric Research* 2020; 231.
- 572 Wu L, Sun Y, Tian Y, Su D. Composition Spectrum of Biogenic Volatile Organic Compounds Released by Typical Flowers in  
573 Beijing. *Environmental Science and Technology* 2014; 37: 154-158.
- 574 Xia C, Xiao L. Estimation of biogenic volatile organic compounds emissions in Jing-Jin-Ji. *Acta Scientiae Circumstantiae*  
575 2019; 39: 2680-2689.
- 576 Yang Y, Wang YH, Zhou PT, Yao D, Ji DS, Sun J, et al. Atmospheric reactivity and oxidation capacity during summer at a  
577 suburban site between Beijing and Tianjin. *Atmospheric Chemistry and Physics* 2020; 20: 8181-8200.
- 578 Yuan ZB, Lau AKH, Shao M, Louie PKK, Liu SC, Zhu T. Source analysis of volatile organic compounds by positive matrix  
579 factorization in urban and rural environments in Beijing. *Journal of Geophysical Research-Atmospheres* 2009;  
580 114: 14.
- 581 Zhu J, Wang S, Zhang S, Xue R, Gu C, Zhou B. Changes in NO<sub>3</sub> Radical and Its Nocturnal Chemistry in Shanghai From 2014  
582 to 2021 Revealed by Long - Term Observation and a Stacking Model: Impact of China's Clean Air Action Plan.  
583 *Journal of Geophysical Research: Atmospheres* 2022; 127.
- 584 Zielinska B, Sagebiel JC, Harshfield G, Gertler AW, Pierson WR. Volatile organic compounds up to C-20 emitted from  
585 motor vehicles; Measurement methods. *Atmospheric Environment* 1996; 30: 2269-2286.
- 586 Zilli M, Palazzi E, Sene L, Converti A, Del Borghi M. Toluene and styrene removal from air in biofilters. *Process*  
587 *Biochemistry* 2001; 37: 423-429.
- 588 Zou Y, Deng X, Li F, Wang B, Tan H, Deng T, et al. Variation characteristics, chemical reactivity and sources of isoprene in  
589 the atmosphere of Guangzhou. *Acta Scientiae Circumstantiae* 2015; 35: 647-655.
- 590